Infrared obscuring potential of selected red phosphorous (RP)/potassium nitrate (KNO₃)-based smoke compositions.

Mohamed Said Goda^{1*}, Mohamed Raafat Ibrahiem⁴, Mohamed Saad Aly³, Ramy Sadek² and Hesham Ramzy Tantawy^{1*}

- ¹ Military Technical College, Cairo, Egypt.
- ² Technical Research Center, Cairo, Egypt.
- ³ National Authority of Military Production, Cairo, Egypt.
- ⁴Benha Faculty of Computers and Artificial Intelligence (BFCAI), Benha, Egypt.

mohamedsaidfadl@gmail.com

Abstract. Thermal imaging systems possess significant civilian and military applications, including the identification of industrial defects, human targets, vehicles, equipment, and weapons systems via the middle (3–5 μm) and far (8–12 μm) infrared bands of the electromagnetic spectrum. This study investigates the obscuring potential of selected red phosphorus (RP)/potassium nitrate (KNO₃)-based pyrotechnic compositions in the far (8–12 μm) infrared band via an image processing technique. Three different compositions, namely K-13, K-16, and K-19, incorporating a constant percentage of 58% red phosphorus, 10% epoxy, and varying percentages of oxidizer (Fe₂O₃) and metallic fuel (magnesium), were investigated. A specially built smoke tunnel coupled with a thermal imager was used to determine the action time, obscuring potential, and impact of compositions on the target image. The composition K-19 with 20% KNO₃, 12% Mg, 58% RP, and 10% epoxy resin by weight demonstrated the maximum performance in terms of rapid action time of 1 second, maximum obscuring potential of 100%, long-lasting obscuration of 60 seconds, and superior performance at obscuration thresholds of 80% and 95% for 53 and 26 seconds, respectively. These findings imply that K-19 serves as a powerful obscurant for sophisticated infrared seekers.

1. Introduction

The electromagnetic spectrum is the complete range of all possible frequencies, each radiation characterized by a certain wavelength and frequency, including the infrared radiation. Infrared radiation arises from molecules and atoms' vibrational and rotational motions and divided to near, middle, and far-infrared wavelengths, as shown in **Figure 1**. Thermal imaging, which observes temperatures for military and civilian applications, uses these three bands of infrared [1, 2].

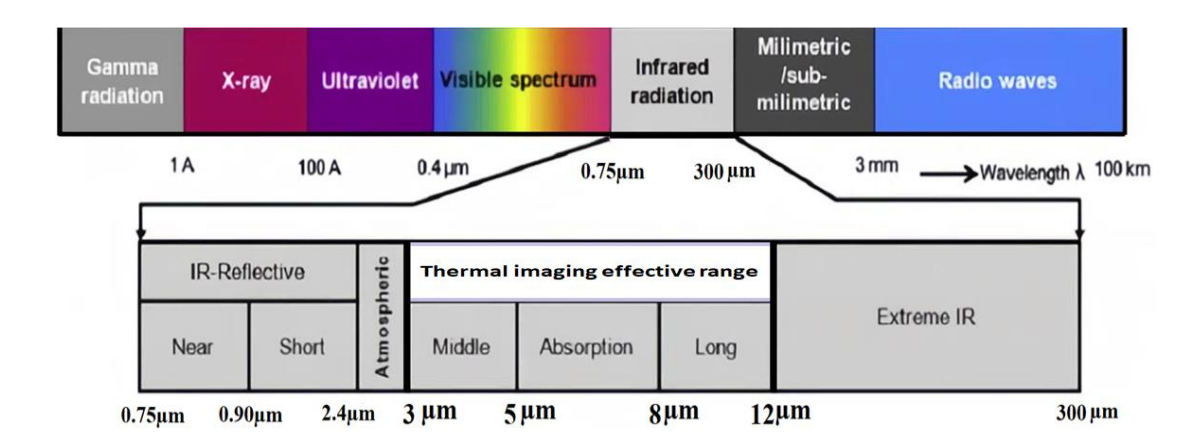


Figure 1. The infrared (IR) region of the electromagnetic spectrum [3].

Thermal imaging technique collects and investigates the thermal data by translating the heat emitted by all objects into graphical representations, which can be applied to static and moving targets, as demonstrated in **Figure 2**. The civilian applications include structure defect detection and industrial inspections, and the military applications involve reconnaissance, surveillance, and target identification, mainly in the mid-infrared (3–5 μ m) and far-infrared (8–12 μ m) spectral bands. Elevated accuracy and sensitivity enable sensor operations within those ranges applied in heat signature detection systems and missile seeker technologies, where thermal imaging is vital in defense operations [4-6].

Infrared seekers and imaging systems have recently been developed to recognize objects with high accuracy using advanced algorithmic datasets. Datasets like deep learning frameworks with multi-kernel transformation, OKTAL-SE-based synthetic databases, and the SENSIAC and Alpha-Beta divergences achieved an accuracy of 97.16% to 98.43%. In conclusion, the average accuracy thresholds for conventional and advanced IR-seekers' recognizing ability are 80% and 95%, respectively [7].

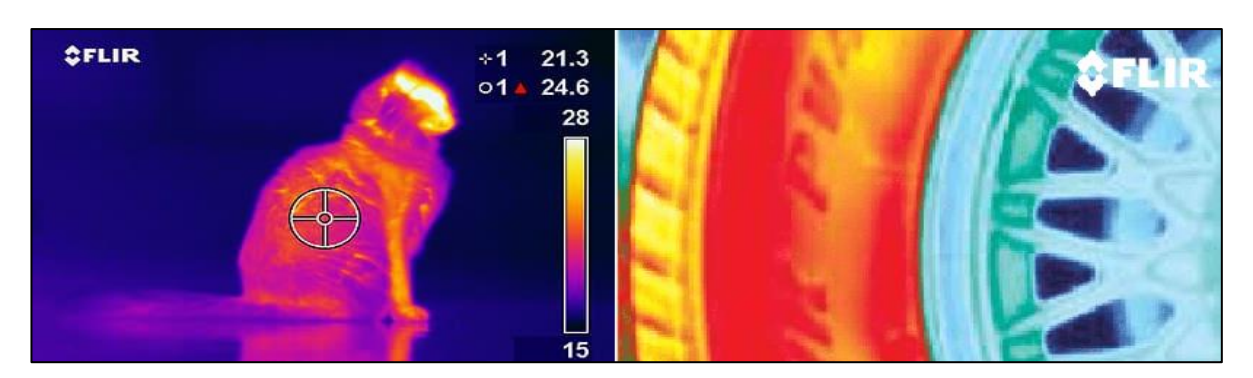


Figure 2. Thermal imaging detection of targets [8].

As a countermeasure, infrared obscurants are employed, often known as military smoke. They disrupt enemy imaging systems operating in the infrared spectrum, particularly in the middle and far-infrared bands. They function via blooming or saturation mechanisms, which expose the sensors to an enormous quantity of infrared radiation. Infrared obscurants also prevent infrared (IR) sensors from detecting, tracking, targeting, or engaging with military forces. Pyrotechnic obscurants consist of non-metallic fuels such as red phosphorus (RP) or anthracene as the primary smoke-generating agents, metallic fuels, oxidizers, and binders [9-11].

Red phosphorus-based smoke compositions are particularly significant due to their infrared attenuation properties; they produce very dense aerosol clouds. When combusted, red phosphorus reacts with atmospheric oxygen to form phosphorus pentoxide, which subsequently absorbs moisture to form

phosphoric acid aerosols. These aerosols efficiently scatter and absorb infrared radiation. Certain RP-based smoke compositions can significantly emit infrared radiation from the smoke cloud, resulting in disruption with infrared sensors. The thermal properties of these smoke compositions make them relevant to military use in screening troop movements and obscuring infrared-guided systems [12-14]. Oxidizers are vital constituents of pyrotechnic compositions. Oxygen-rich compounds release oxygen gas by decomposing at specific temperatures. This released oxygen supports the combustion of fuels in generating airborne obscurants for infrared attenuation purposes. Common oxidizing agents include nitrates, chlorates, perchlorates, and metal oxides; the choice of oxidizer depends upon several considerations, such as reactivity, thermal stability, and compatibility with fuel. The careful selection and preparation of such oxidizers are crucial for better performance with significantly enhanced safety during storage and applications [15]. Potassium nitrate (KNO₃) is a strong oxidizing agent. It also has a high (39.6%) active oxygen content and decomposes at high temperatures through a strongly endothermic reaction to achieve rapid burning rates [16].

Fuels are powdered materials that react with oxidizers to produce various pyrotechnic effects, such as sound, light, color, heat, and smoke. Metallic fuels include magnesium and aluminum; non-metallic fuels include carbon, sulfur, and phosphorus. Magnesium is a significant metallic fuel in various pyrotechnic mixtures. It reacts rapidly and burns well, and due to its high thermal conductivity, it enhances the propagation of burning. Furthermore, it reacts rapidly with oxygen and releases a significant amount of thermal energy [17, 18].

Binders provide mixtures with mechanical strength to avoid physical degradation. Binders hold the pyrotechnic mixtures' components in a homogeneous blend. Natural binders typically used in pyrotechnics are (paraffin wax and beeswax) while common synthetic binders are (butyl rubber, polyester, polyvinyl chloride, and epoxy resin) [19].

This study investigates the obscuring potential of selected RP/KNO₃-based smoke compositions in the far-infrared band. The study aims to determine the most effective smoke composition in terms of minimum action time, maximum obscuring potential, and impact on the monitored target image. Red phosphorus serves as the smoke-generating substance, magnesium serves as the metallic fuel, potassium nitrate serves as the oxidizer, and epoxy resin serves as the binder. The binder and RP will be fixed at 10% and 58% by weight of the total mixture, while oxidizer and metallic fuel will be variables at the expense of each other.

2. Materials and method

2.1. Chemicals and Sample Preparation

All the chemicals were commercial grade. They were employed after the sieving process to achieve the desired particle size below 100 μm . The selected chemicals are listed in **Table 1**.

No.	Chemical compounds	Chemical formula	M.wt (g/mol)	Purity	Origin
1	Red phosphorus	P_4	30.97	98 %	Jiangsu, China
2	Potassium nitrate	KNO_3	101.1	99.8 %	Shandong, China
3	Magnesium	Mg	24.31	99.8 %	Shanxi, China
4	Epoxy	$[-(C_{28}H_{30}O_2)-]n$	398.54	98 %	Guangdong, China
5	Trichloroethylene	C ₂ HCl ₃	131.4	99.9%	Guangdong, China

Table 1. List of chemicals.

The powdered raw ingredients were sieved and then mixed with trichloroethylene solvent to form a paste, which was pressed into the form of disc and left to dry. We obtained a dried mixture pressed for testing. The investigation focused on three compositions. **Table 2** displays the studied percentages by weight of RP/KNO₃-based smoke compositions.

Table 2. RP/KNO₃-based smoke compositions.

No.	Code		Components (wt.%)			
		RP	Mg	KNO_3	Epoxy	
1	K-13	58	24	8	10	
2	K-16	58	18	14	10	
3	K-19	58	12	20	10	

2.2. Experimental setup and evaluation

The experimental setup consisted of a black body radiator model (ECN 100), thermal imager Fluke tix-580 (8–12 μ m), and recorders for gathering data. A specifically built smoke tunnel was employed to analyze and appraise the obscuring potential of the RP/KNO₃-based smoke compositions. The detailed specifications and dimensions of the smoke tunnel are shown in **Table 3**. The smoke tunnel was outfitted with suction blower and measuring sensors, determining relative humidity, temperature, and wind speed. Additionally, a control unit regulates the wind speed inside the smoke tunnel. The smoke was produced by the electrical ignition of smoke compositions using a squib inside the smoke production chamber.

Table 3. Specification of the used smoke tunnel.

Item	Specification
Material	Stainless Steel
Diameter	1 m
Cross-section	0.785 m^2
Length	9 m
Air velocity	(0.5-5) m/s
Total volume	7.065 m^3
Suction blower power	2 hp

The infrared black body radiator was positioned at a specified location on the tunnel side to mimic the field target under observation. The thermal imager and its associated recording and processing equipment were on the opposite side of the test section, as shown in **Figure 3**. The infrared radiation attenuation from the black body radiator caused by each smoke sample was recorded, graphed, and analyzed over time.

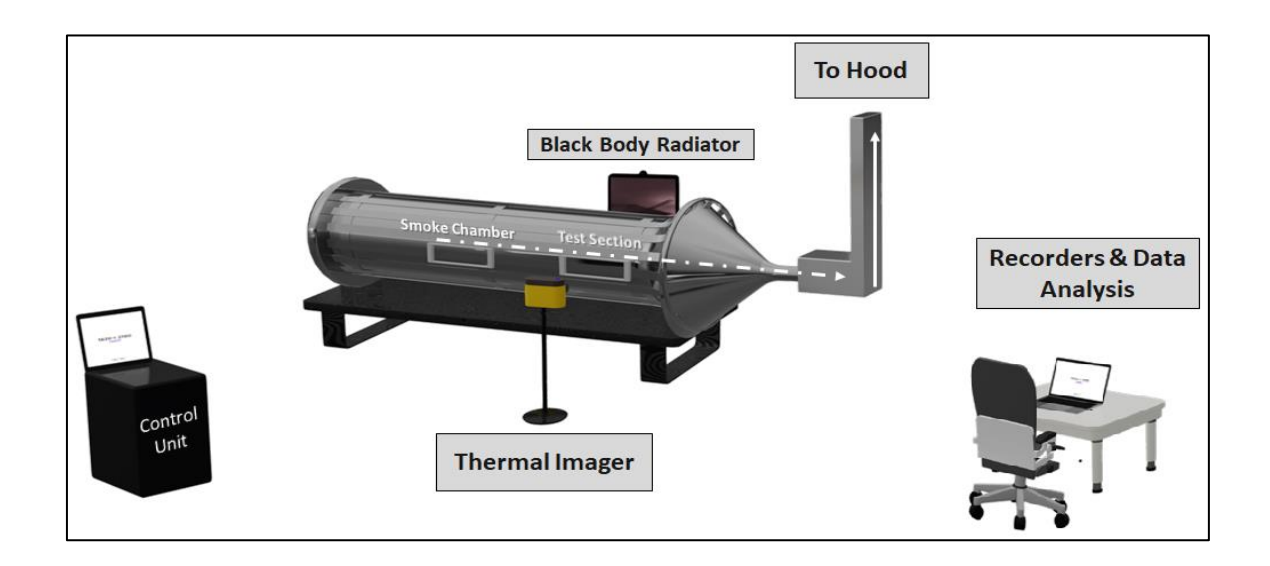


Figure 3. Full schematic diagram of the smoke tunnel and the equipment setup.

Video recordings obtained from the thermal imager were analyzed through an advanced programming language, including Python and Visual Studio Code. The primary objective of these software packages is to measure the thermal obscuring potential of the RP/KNO₃-based smoke compositions using image processing techniques. The method involved capturing images at set intervals and then selecting the target temperature in the original image as reference before smoke production with 100°C for target temperature at an air flow speed of 1 m/s.

3. Results and discussions

K-13, K-16, and K-19 were comprehensively analyzed to highlight the smoke cloud's significant impact on the monitored target image due to the infrared radiation emission, scattering, and absorption. **Figure 4** shows the Fluctuation of the far-infrared obscuring potential of K-13, K-16, and K-19 over time, as recorded by the thermal imager. **Table 4** lists their integrated area under the curve, while **Figure 5** demonstrate the thermal images visual inspection to verify the performance superiority of K-19.

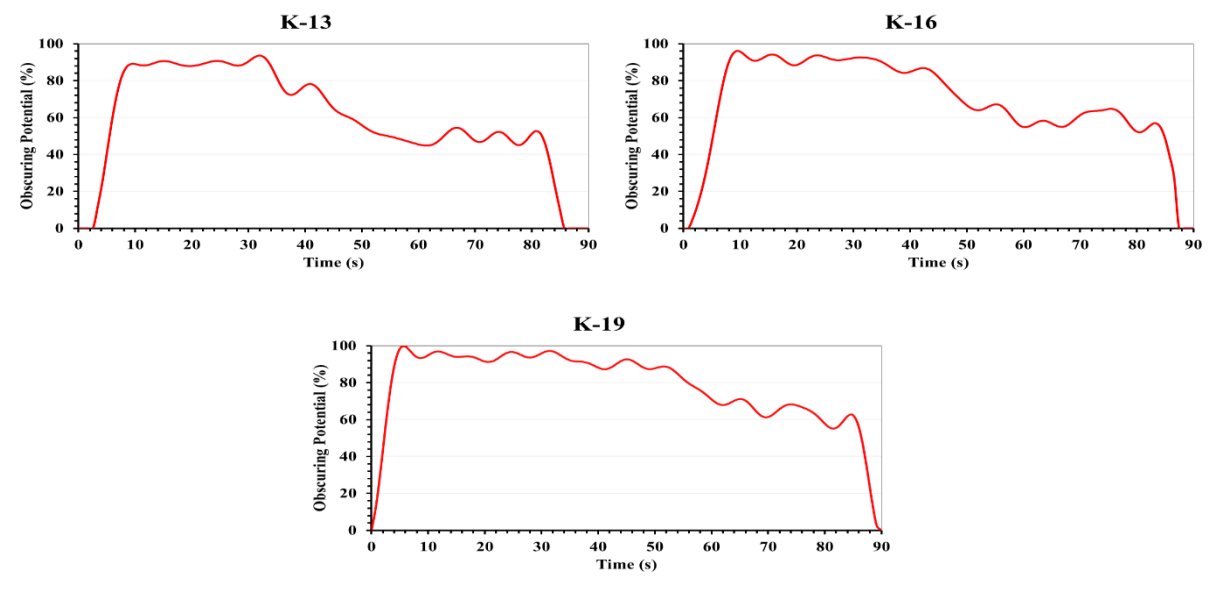


Figure 4. The fluctuation of the far-IR obscuring potential of K-13, K-16, and K-19 over time.

Table 4. Integrated area under the curve of K-13, K-16, and K-19.

Composition	Area under the curve
K-13	5381
K-16	6178
K -19	7060

K-13 and K-16 exhibit action times of approximately 2.5 and 1.5 seconds, with the image beginning to fade after 6 and 5 seconds, respectively. K-13 and K-16 achieved complete obscuration of 90 and 96% after 8 and 9 seconds of ignition, respectively. The obscuration of K-13 remains for 35, marking the shortest duration, while K-16 obscuration remains for 41. Partial image recovery of K-13 and K-16 occurred at 50 and 60 seconds, and full recovery was observed at 85 and 87 seconds, respectively. K-19 demonstrated a rapid action time of 1 second, with the image fading to an unrecognizable state after 2.5 seconds. Complete obscuration of 100% was achieved 6 seconds after ignition, with a successful and prolonged duration of 60 seconds. Partial image recovery occurred at 70 seconds, followed by full recovery at 90 seconds.

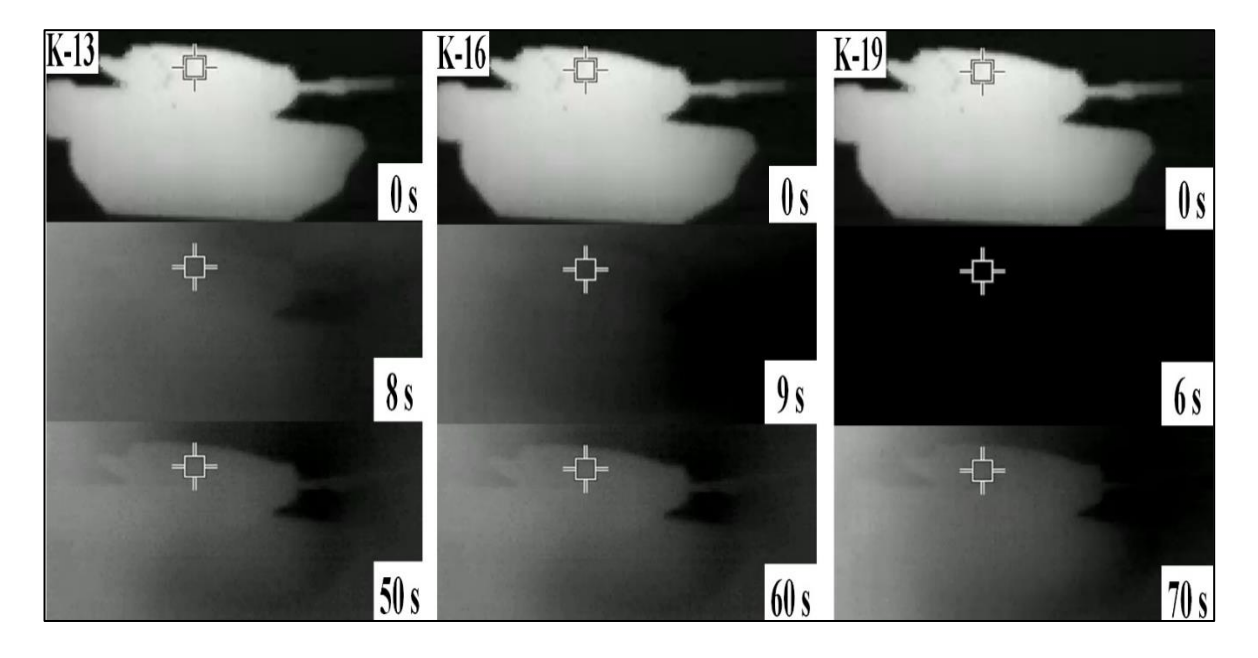


Figure 5. Effects of the K-13, K-16, and K-19 smoke clouds on the monitored target image over time.

These findings align with the image pixel mode (**Figure 6**), indicating the superiority of K-19. It offers the shortest action time required to affect the target image, the highest level of obscuring potential at 100%, and a successful obscuring duration of roughly 60 seconds, which is the longest duration compared to K-13 and K-16.

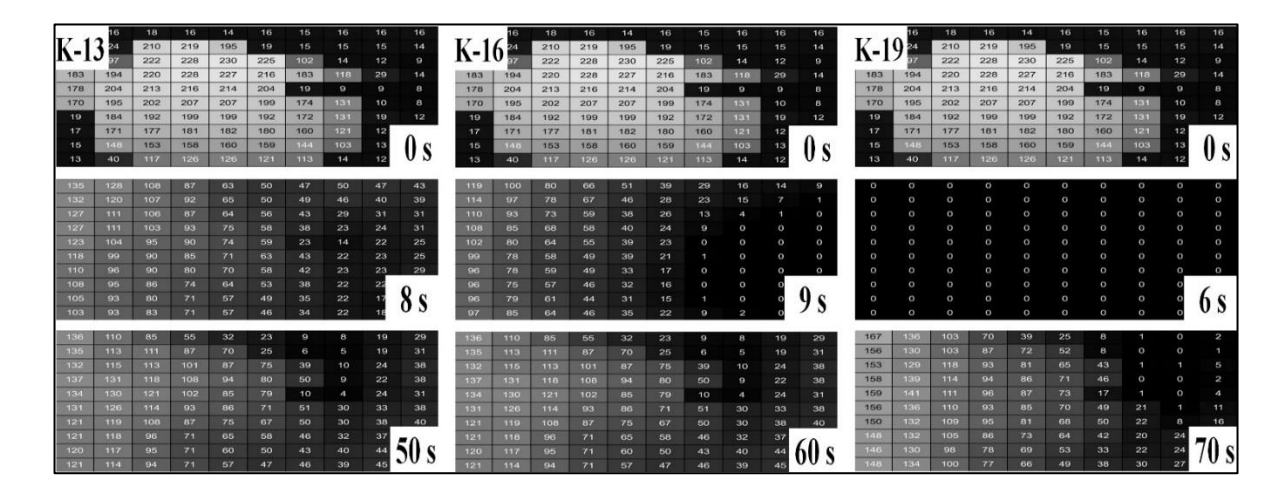


Figure 6. Effect of the K-13, K-16, and K-19 smoke clouds on the monitored target image over time (Pixel Mode).

Table 5. summarizes the study results and illustrates the superiority of K-19 in terms of action time, obscuring potential, duration, and obscuration time.

Table 5 . Obscuration	performance	observations	of K-13,	K-16,	and K-19.
------------------------------	-------------	--------------	----------	-------	-----------

Composition	Action Time (s)	Maximum Obscuring Potential (%)	Obscuration Time (s)	Duration Time (s)
K-13	2.5	90	35	85
K-16	1.5	96	41	87
K-19	1	100	60	90

Figure 7. illustrates the variations in far-IR obscuration time for K-13, K-16, and K-19 at varying obscuration thresholds of 80% and 95%. K-19 exhibits maximum durations of 53 and 26 seconds for both 80% and 95% obscuration thresholds, respectively, indicating a composition-dependent peak in efficiency. These findings suggest that composition K-19 is a viable candidate for both conventional and advanced infrared seeker countermeasures.

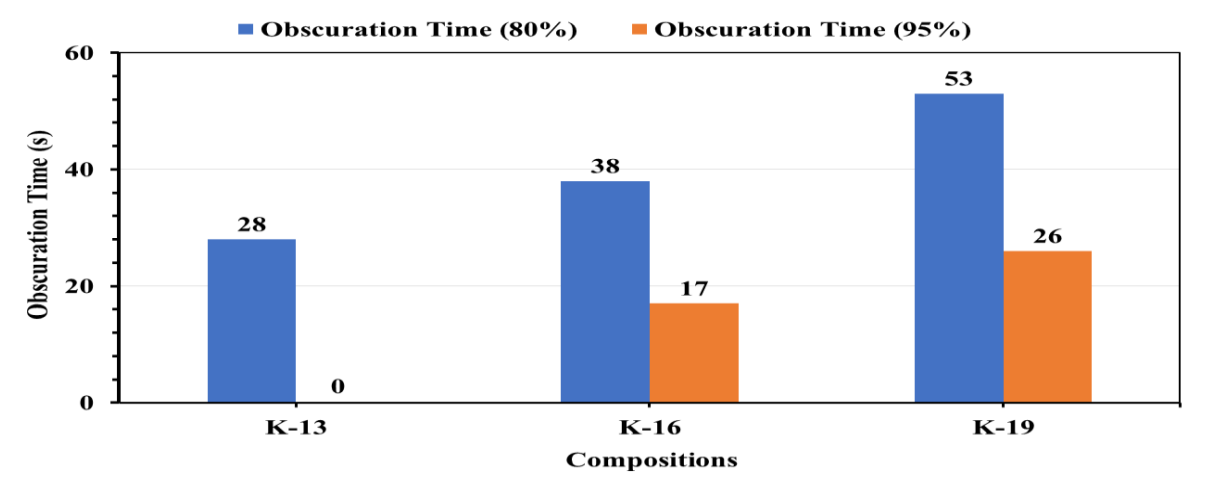


Figure 7. Variations in far-IR obscuration time for K-13, K-16, and K-19 at varying obscuration thresholds of 80% and 95%.

4. Conclusion

This investigation aimed to determine whether specific RP/KNO₃-based pyrotechnic compositions were competent in achieving a rapid action time, maximum obscuration time, and maximum obscuring potential in the far infrared spectral band (8–12 µm). Red phosphorus, magnesium, potassium nitrate, and epoxy resin were the selected constituents of the smoke compositions under investigation. The impact of the produced smoke cloud on the target image obscuration performance was evaluated via image processing technique. Composition K-19 with 20% KNO₃, 12% Mg, 58% RP, and 10% epoxy resin by weight achieved an optimal infrared obscuration performance surpassing K-13 and K-16. K-19 had the shortest action time of 1s with highest obscuring potential and the most extended obscuration time of 60 seconds. Its performance sustained at varying obscuration thresholds of 80% and 95% for 53 and 26 seconds, respectively. These findings indicate the potential of K-19 as a promising candidate and reliable smoke composition countermeasure against infrared seekers.

References

- [1] Y.-i. Hayashi, "State-of-the-art research on electromagnetic information security," *Radio Science*, vol. **51**, no. 7, pp. 1213-1219, 2016.
- [2] G. C. Holst and D. P. Haefner, "Infrared Imaging Systems: Design, Analysis, Modeling, and Testing XXXIV," in *Proc. of SPIE* Vol, 2023, vol. **12533**, pp. 1253301-1.
- [3] A. K. Abbas, K. Heimann, V. Blazek, T. Orlikowsky, and S. Leonhardt, "Neonatal infrared thermography imaging: analysis of heat flux during different clinical scenarios," *Infrared Physics & Technology*, vol. **55**, no. 6, pp. 538-548, 2012.
- [4] R. A. Osornio-Rios, J. A. Antonino-Daviu, and R. de Jesus Romero-Troncoso, "Recent industrial applications of infrared thermography: A review," *IEEE transactions on industrial informatics*, vol. **15**, no. 2, pp. 615-625, 2018.
- [5] R. N. Strickland, "Infrared techniques for military applications," in *Infrared Methodology and Technology*: CRC Press, 2023, pp. 397-427.
- [6] P. J. Kemper Jr and J. S. DiMarco, "Imaging infrared seeker signal processing overview: image processing, adaptive thresholding, and track processing," in *Infrared Imaging Systems: Design, Analysis, Modeling, and Testing X*, 1999, vol. **3701**: SPIE, pp. 266-273.
- [7] L. Xu, F. Zhao, P. Xu, and B. Cao, "Infrared target recognition with deep learning algorithms," *Multimedia Tools and Applications*, vol. **82**, no. 11, pp. 17213-17230, 2023/05/01 2023, doi: 10.1007/s11042-022-14142-x.
- [8] F. Company. "The Thermogram of a domestic cat and a spinning car tire." https://covalentmetrology.com/service/infrared-thermography-irt/ (accessed.
- [9] G. Pulpea *et al.*, "Thermal systems capabilities using infrared obscurants," *Journal of Optoelectronics and Advanced Materials*, vol. **19**, no. January-February 2017, pp. 16-26, 2017.
- [10] K. v. Stackleberg, T. S. Smith, D. M. Cropek, B. A. MacAllister, and C. Amos, "Military smokes and obscurants fate and effects: a literature review relative to threatened and endangered species," 2004.
- [11] S. Cudziło, "Studies of IR-Screening Smoke Clouds," *Propellants, Explosives, Pyrotechnics*, vol. **26**, no. 1, pp. 12-16, 2001.
- [12] S. D. Quang, T. N. Van, and T. N. Trung, "Obscurant and radiation characteristics of infrared-screening smoke composition based on red phosphorus," *Defence Science Journal*, vol. **72**, no. 3, pp. 353-358, 2022.
- [13] M. Somayajulu, G. Gautam, S. Jayaraman, and J. Agrawal, "Studies on characterization and burning of red phosphorus-based smoke compositions," *Journal of energetic materials*, vol. **21**, no. 1, pp. 15-31, 2003.
- [14] Y. Suzuki, K. Matsunaga, and Y. Suzuki, "IR-Screening properties of red phosphorus smoke," *Kayaku Gakkaishi*, vol. **63**, no. 4, pp. 185-190, 2002.
- [15] A. Q. Malik, "Thermal and kinetic comparison of various oxidizers used in propellant/pyrotechnic compositions," *Caspian Journal of Applied Sciences Research*, vol. **2**, no. 7, 2013.

- [16] S. V. Levchik, G. F. Levchik, G. Camino, L. Costa, and A. I. Lesnikovich, "Fire-retardant action of potassium nitrate in polyamide 6," *Die Angewandte Makromolekulare Chemie: Applied Macromolecular Chemistry and Physics*, vol. **245**, no. 1, pp. 23-35, 1997.
- [17] Z. Babar and A. Q. Malik, "Thermal decomposition, ignition and kinetic evaluation of magnesium and aluminium fuelled pyrotechnic compositions," *Central European Journal of Energetic Materials*, vol. **12**, no. 3, 2015.
- [18] S. Pourmortazavi, S. Hajimirsadeghi, I. Kohsari, M. Fathollahi, and S. Hosseini, "Thermal decomposition of pyrotechnic mixtures containing either aluminum or magnesium powder as fuel," *Fuel*, vol. **87**, no. 2, pp. 244-251, 2008.
- [19] A. Khan, A. Q. Malik, Z. H. Lodhi, and G. Badshah, "Study of effect of binders and loading pressures on the performance of the time delay pyrotechnic compositions," *Journal of Energetic Materials*, vol. **36**, no. 4, pp. 386-397, 2018.